

Identifying nearby sources of ultra-high-energy cosmic rays with deep learning

Oleg Kalashev,^{a,b} Maxim Pshirkov,^{a,c,d} Mikhail Zotov^e

^aInstitute for Nuclear Research of the Russian Academy of Sciences, Moscow, 117312, Russia

^bMoscow Institute for Physics and Technology, 9 Institutskiy per., Dolgoprudny, Moscow Region, 141701 Russia

^cSternberg Astronomical Institute, Lomonosov Moscow State University, Moscow, 119992, Russia

^dLebedev Physical Institute, Pushchino Radio Astronomy Observatory, 142290, Russia

^eSkobeltsyn Institute of Nuclear Physics, Lomonosov Moscow State University, Moscow, 119991, Russia

E-mail: kalashev@inr.ac.ru, pshirkov@sai.msu.ru, zotov@eas.sinp.msu.ru

Abstract. We present a method to analyse arrival directions of ultra-high-energy cosmic rays (UHECRs) using a classifier defined by a deep convolutional neural network trained on a HEALPix grid. To illustrate the efficacy of the method, we employ it to estimate prospects of detecting a large-scale anisotropy of UHECRs induced by a nearby source with an (orbital) detector having a uniform exposure of the celestial sphere and compare the results with our earlier calculations based on the angular power spectrum. A minimal model for extragalactic cosmic rays and neutrinos by Kachelrieß, Kalashev, Ostapchenko and Semikoz (2017) is assumed for definiteness and nearby active galactic nuclei Centaurus A, M82, NGC 253, M87 and Fornax A are considered as possible sources of UHECRs. We demonstrate that the proposed method drastically improves sensitivity of an experiment by decreasing the minimal required amount of detected UHECRs or the minimal detectable fraction of from-source events several times compared to the approach based on the angular power spectrum. The method can be readily applied to the analysis of data of the Telescope Array, the Pierre Auger Observatory and other cosmic ray experiments.

Keywords: ultra-high-energy cosmic rays, anisotropy, active galactic nucleus, cosmic ray experiments, deep learning, convolutional neural network, simulations

Contents

1	Introduction	1
2	Traditional approach	2
3	Neural network classifier based on the angular power spectrum	4
4	Deep convolutional classifier	5
5	Conclusions	8

1 Introduction

Cosmic rays of the highest energies ($E \gtrsim 50$ EeV, ultra-high-energy cosmic rays, UHECRs) were first detected more than 60 years ago [1] and still remain at the forefront of the high energy astrophysics. Due to the limited distance of CRs propagation at these energies amounting to ~ 100 Mpc, a certain degree of anisotropy is expected in the distribution of their arrival directions. The level of an anisotropy and its other properties depend on characteristics of sources of UHECRs, thus study of the anisotropy is one of the key parts of this branch of astrophysics.

Studies of an anisotropy of CR arrival directions are only feasible when a sufficiently large amount of data is available. Due to the extremely low flux of UHECRs, obtaining the required number of events demands instruments with a very large exposure. One of possible solutions of the problem is employing space-born detectors, which observe UV-radiation from extensive air showers induced by UHECRs in the Earth's atmosphere. Several missions of the kind are under development now, such as KLYPVE-EUSO (K-EUSO) [2–5] and POEMMA [6, 7]. In our previous paper [8], we studied sensitivity of these future orbital missions to a large-scale anisotropy emerging due to the presence of a nearby source. A particular model for cosmic rays and neutrinos by Kachelrie, Kalashev, Ostapchenko and Semikoz (KKOS in what follows) [9], which can act as a representative of a broader class of models, was selected for the analysis. The model assumes that UHECRs are accelerated by (a subclass of) active galactic nuclei (AGN) with the energy spectra of nuclei following a power-law with a rigidity-dependent cut-off after the acceleration phase. The model successfully reproduces the energy spectrum of cosmic rays with energies beyond 10^{17} eV registered with the Pierre Auger Observatory and the spectrum of high-energy neutrinos registered by IceCube, as well as data on the depth of maximum of air showers X_{\max} and $\text{RMS}(X_{\max})$. One of the consequences of the model is the existence of a nearby (within ~ 20 Mpc) AGN acting as a source of UHECRs. Presence of such an accelerator would inevitably lead to deviations from isotropy at some level and produce detectable imprints on the angular power spectrum (APS) of the UHECR flux providing the fraction of nuclei arriving from the source is sufficiently high. We considered five nearby AGN

often discussed in literature as possible sources of UHECRs and demonstrated that an observation of $\gtrsim 200$ – 300 events with energies $\gtrsim 57$ EeV will allow detecting deviations from isotropy with a high level of statistical significance if the fraction of events from any of these sources is $\simeq 10$ – 15% of the total flux.

Use of the APS allows for a very robust approach to an analysis of anisotropy but has certain drawbacks since some information such as the characteristic shape and size of a region with an excessive flux of UHECRs produced by the source are only partially preserved in the APS coefficients. That results in a somewhat lower sensitivity to a sought signal. In the present paper, we searched for this signal exploiting all available information about arrival directions of UHECRs. To do that, we employed two approaches widely used in machine learning: the simplest possible neural network classifier consisting of a single sigmoid perceptron and a convolutional neural network (CNN) classifier trained on a HEALPix grid. Both types of neural networks have demonstrated their efficacy in a wide range of problems related to classification of data and pattern recognition, see, e.g., [10] for a brief introduction.

In what follows, we consider the two neural networks and demonstrate that even the simplest of them allows improving the results obtained within the traditional approach but the CNN presents a real breakthrough by reducing the number of events needed for establishing an anisotropy of UHECRs from a nearby source 2–4 times or strongly decreasing the necessary level of the flux of events arriving from the source.

2 Traditional approach

Let us briefly remind the key points of our earlier work based on calculating the angular power spectrum of CR arrival directions [8], which mostly followed a method suggested by the IceCube and the Pierre Auger Observatory collaborations [11, 12]. We considered five nearby active galactic nuclei Centaurus A, M82, NGC 253, M87 and Fornax A as possible sources of UHECRs. All of them are located within a sphere with a radius of ~ 20 Mpc with the first three being as close as 3.5–4 Mpc from the Galaxy. For the aims of the analysis, we generated multiple sets of mock maps imitating arrival directions of nuclei coming from these sources.

In a simplified approach of the KKOS model, all sources share the same injection spectrum and composition. These properties were found from the global fit of the CR spectrum and composition observed at Earth. However, both composition and spectrum evolve during propagation of nuclei in the inter-galactic media. That was taken into account with the TransportCR code [13]. We only considered nuclei with energies above 57 EeV, and this allowed us to assume the extragalactic magnetic fields do not strongly deflect the nuclei [14] so that UHECRs arrive to the Milky Way within $\pm 1^\circ$ from the original direction. Next we employed the CRPropa 3 code [15] to simulate propagation of nuclei in the Galactic magnetic field, for which we assumed the Jansson–Farrar model [16]. All three components of the magnetic field present in the model (the regular, striated and turbulent ones) were utilised in simulations. The calculations were performed on the HEALPix¹ grid with $N_{\text{side}} = 512$. The corresponding angular

¹<https://healpix.sourceforge.io>

resolution of the grid (7') is much higher than the angular resolution of any of the existing or forthcoming cosmic ray experiments but it allowed us to obtain an accurate sampling of arrival directions of from-source UHECRs.

Having these tools, it is straightforward to produce a map of arrival directions of N UHECRs, N_{src} of which come from a particular source. The procedure is as follows. One takes the propagated spectrum calculated with TransportCR for a source located at a given distance from the Galaxy and samples it N_{src} times, each time extracting some nuclei with an energy E and charge Z . An observed arrival direction of a cosmic ray is found then for each (E, Z) pair (or, equivalently, for each rigidity) using the mapping obtained with CRPropa by backpropagation. Finally, the remaining $N - N_{\text{src}}$ events are generated following the isotropic distribution. The whole process is repeated multiple times in order to generate a large number of maps for each source.

After that, we prepared maps of the relative intensity of the CR flux and calculated their angular power spectra looking for the minimal fraction η of from-source events in the whole sample allowing one to reject the null hypothesis of an isotropic distribution at a high confidence level. The hypothesis of isotropy was tested using the following estimator:

$$D(\text{sample}) = \frac{1}{\ell_{\text{max}}} \sum_{\ell=1}^{\ell_{\text{max}}} \frac{C_{\ell, \text{sample}} - \langle C_{\ell, \text{iso}} \rangle}{\sigma_{\ell, \text{iso}}}, \quad (2.1)$$

where “sample” is either “mix” when applied to samples that contain a contribution from an UHECR source, or “iso” when applied to isotropic samples, and C_{ℓ} are coefficients of the angular power spectrum:

$$C_{\ell} = \frac{1}{2\ell + 1} \sum_{m=-\ell}^{+\ell} |a_{\ell m}|^2. \quad (2.2)$$

Thus, variables $C_{\ell, \text{sample}}$, $\langle C_{\ell, \text{iso}} \rangle$ and $\sigma_{\ell, \text{iso}}$ in Eq. (2.1) are respectively the C_{ℓ} observed in the sample (either “mix” or “iso”), the average and the standard deviation of C_{ℓ} for isotropic expectations, all of them calculated at a given scale ℓ . Coefficients $a_{\ell m}$ in Eq. (2.2) are the multipolar moments of the spherical harmonics used to decompose the relative intensity of the flux.

Since both $D(\text{iso})$ and $D(\text{mix})$ in Eq. (2.1) are random variables, one needs to compare their distributions. It was assumed as the null hypothesis that arrival directions of a mixed sample of UHECRs obey an isotropic distribution. We adopted the value of the error of the second kind (the probability not to reject the null hypothesis when it is false) $\beta = 0.05$ and searched for a minimal fraction η of from-source events in the total flux such that the error of the first kind (the probability to reject the true null hypothesis) $\alpha \lesssim 0.01$. For the sake of uniformity, all calculations of the estimator D presented in [8] were performed with $\ell_{\text{max}} = 16$ though it was remarked that the choice is not necessarily optimal, and slightly better results can be obtained by adjusting ℓ_{max} for each particular source, depending on its angular power spectrum.

Calculations were performed for samples of sizes $N = 100, 200, \dots, 500$ to cover

the whole possible range of UHECRs to be detected by K-EUSO above 57 EeV [4].² The main result of [8] is presented in Table 1 (for $N \geq 100$).

Table 1. Percentage of UHECRs arriving from five candidate sources in samples of sizes $N = 50, 100, \dots, 500$ such that the error of the first kind $\alpha \lesssim 0.01$ for the null hypothesis of isotropy providing the second kind error $\beta = 0.05$. The accuracy of the numbers is ± 1 for $N > 100$ and ± 2 otherwise. The result was obtained with fixed $\ell_{\max} = 16$.

N	50	100	200	300	400	500
NGC 253	24	17	12	10	8	7
Cen A	28	21	14	12	10	9
M82	36	26	18	14	12	11
M87	38	29	20	16	14	12
Fornax A	28	19	13	11	9	8

Adjusting ℓ_{\max} to minimize η allows decreasing numbers shown in Table 1 by a few percent (from 2–6% for $N = 50$ to 1–2% for $N = 500$) most notably for Cen A and Fornax A, for which a deviation of the lower multipoles from the isotropic distribution is most pronounced, see [8]. Obviously, this does not present a noticeable improvement of the result.

We remark the KKOS model provides a heavy mass composition of UHECRs at energies above 57 EeV thus resulting in much more fuzzy patterns of arrival directions if compared with the case of a light (mostly proton and Helium) composition. In this sense, our results are conservative since having more compact patterns will allow one to obtain less restrictive demands on the minimal number of from-source events needed to reject the isotropy hypothesis.

3 Neural network classifier based on the angular power spectrum

As the first step, we tried to obtain a better estimator based solely on the APS coefficients C_ℓ . We trained the simplest possible neural network classifier consisting of a single sigmoid perceptron, which defines the test statistics ξ as

$$\xi = \sigma \left(\sum_{\ell=0}^{\ell_{\max}} w_\ell C_\ell \right), \quad (3.1)$$

where σ is the sigmoid function (sometimes called the logistic function) and w_ℓ are weights corresponding to the angular scale ℓ .

We limited the maximum value of ℓ by $\ell_{\max} = 32$ and trained the classifier on the set of 50K samples with the total number of events $N = 500$ and a random admixture of events from Cen A ranging from 1 up to 500 sampled uniformly in log scale, plus 50K

²While the article was focused on K-EUSO, its results are true for any other detector with a uniform exposure of the celestial sphere.

samples generated from the purely isotropic distribution. We used the cross-entropy as the loss function assuming the target value of 1 for all samples with an admixture of from-source events and 0 otherwise [10].

The weights were optimized using the Adadelta adaptive learning rate method [17]. The optimization was performed for 2000 epochs with the conditional early stop, i.e., until the loss function on the validation data was not improving for more than 50 epochs. The learned weights w_ℓ are shown in Fig. 1. It is clear from the figure that not all values of C_ℓ are equally important for the classification task. This makes a crucial difference with the traditional approach described in Section 2, which assumes all multipoles are considered on the equal basis (with “equal weights” in the machine learning parlance). The most important range of ℓ is $1 \leq \ell \leq 5$ with the maximum weight at $\ell = 2$, which is obviously different from the range used in the previous study.³

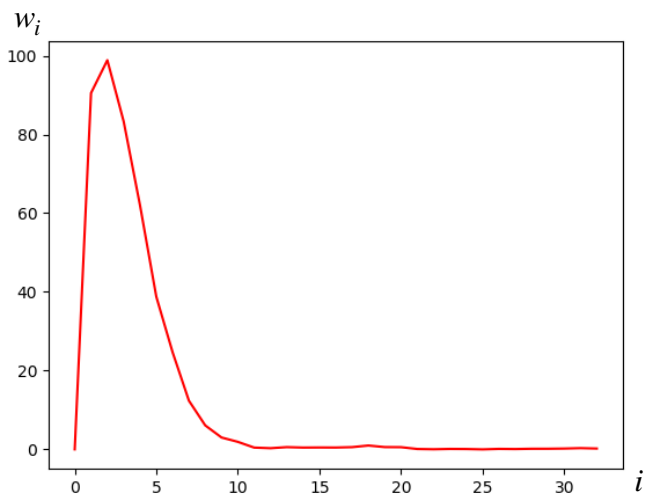


Figure 1. Sigmoid perceptron weights as defined in Eq. (3.1) after training on the angular power spectrum generated assuming an admixture of events from Cen A for $N = 500$.

Applying this simplest neural network allowed us to slightly improve results obtained with the traditional approach. The minimal detectable fraction η of events arriving from Cen A was found to be 4% compared to 9% (or 6.4% after adjusting ℓ_{\max}) for $N = 500$, and 20% compared to 28% (22% after adjusting ℓ_{\max}) for $N = 50$. We remark that training and testing the neural network demanded considerable computational resources.

4 Deep convolutional classifier

As we have already mentioned above, a classifier based solely on the angular power spectrum can not benefit from information about a pattern of arrival directions of UHECRs coming from a particular source. An obvious way to overcome this limitation

³Adjusting ℓ_{\max} to minimize η within the traditional approach leads to $\ell_{\max} = 5$ in this particular case.

is to use an arrival direction map as an input to the neural network classifier. In what follows, we use a convolutional neural network architecture [18], a widely used subclass of feed-forward neural networks designed specifically for pattern recognition and image classification tasks.

The basic idea behind CNNs is using local feature maps at different scales to extract valuable information and perform a classification task. A variety of CNN implementations exist for many programming languages and platforms. However, most of them support operations on flat (two-dimensional) images only. A number of implementations for convolutional operations on the sphere were proposed recently [19–21]. We employed the publicly available code developed by Krachmalnicoff and Tomasi [21], which implements convolution and pooling (down-sampling) operations on the HEALPix grid data with the help of Keras deep learning library [22]. The convolution operation on the HEALPix grid is parameterized by 9 adjustable weights per feature map. The CNN architecture developed in this work is shown in Fig. 2. The training and validation sets were prepared in the same way as in Section 3.

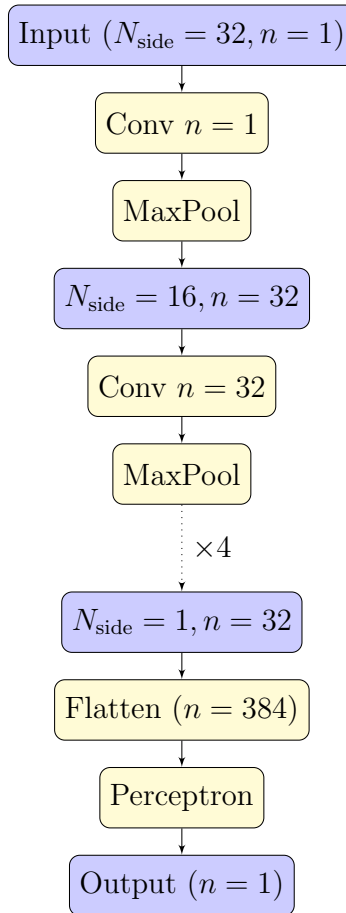


Figure 2. Architecture of the CNN developed in this work. Blue boxes are used to show feature vectors and maps. Yellow boxes show operations.

The network takes one feature map ($n = 1$ in Fig. 2) in the HEALPix grid with

$N_{\text{side}} = 32$ as an input. Thirty-two feature maps ($n = 32$) are built at the first step using the convolution operation with 32×9 free parameters and max-pooling the image to $N_{\text{side}} = 16$. The sequence of convolutions and max-pooling operations is repeated until reaching $N_{\text{side}} = 1$ with the persistent number of feature maps, which means that each intermediate convolution operation has $32 \times 32 \times 9$ trainable weights. The rectified linear activation function (ReLU) is used for all intermediate layers. Finally, 32 feature maps with $N_{\text{side}} = 1$ are flattened and sent to a single-layer sigmoid perceptron. To avoid overfitting, we use an early-stop technique. Namely, we train our model for at most 1000 epochs and interrupt training in case accuracy on validation data is not improving for 10 epochs. Attempts to use other regularization techniques, such as dropout and the L2 regularization demonstrated little benefit. The output of the classifier, a number between 0 and 1 was used as test statistics. The minimal fractions η of from-source UHECRs needed to reject the null hypothesis of an isotropic flux with the same demands on α and β as above, are shown in Table 2.

Table 2. Fractions of from-source UHECRs defined as in Table 1 but obtained using a test statistics based on the CNN classifier.

N	50	100	200	300	400	500
NGC 253	8	4	2.5	2	1.75	1.2
Cen A	10	6	4	2.7	2.5	2
M82	14	8	4.5	3.6	3	2.4
M87	16	9	5	3.3	2.5	2.4
Fornax A	10	5	3	2.3	2	1.6

Notice the minimal fractions of from-source events needed to find an anisotropy decreased drastically in comparison with those presented in Table 1, so that registering just 50 events over the whole celestial sphere is needed providing any of the five sources generates ~ 10 – 15% of the total flux. More than this, the minimum necessary size of the total data sample can be lowered down to 40 events for Cen A, NGC 253 and Fornax A. This means even a pattern like the one shown in Figure 3 with mere five UHECRs coming from Fornax A and 35 forming the isotropic background can be recognized by the CNN. Alternatively, a tiny fraction of UHECRs from any of the five sources can be identified with a larger sample of experimental data.

We also tried to use more dense maps with $N_{\text{side}} = 64, 128$ for the classifier input and found that the minimal detectable fraction only moderately depends on N_{side} for $N_{\text{side}} \geq 32$ but grows substantially for $N_{\text{side}} \leq 16$ maps.

Remark. It was considered in [8] if an anisotropy arising from a nearby source at energies above 57 EeV can be found by the existing experiments at lower energies. It was demonstrated that the fraction of from-source events scales almost linearly down to energies $\gtrsim 3$ EeV, and there is very little difference between sources located at distances 3.5 Mpc and 20 Mpc. As a result, a source providing 10–15% of the flux beyond 57 EeV can only contribute 1–1.5% at energies above 8 EeV, at which a dipole anisotropy was found by the Pierre Auger collaboration [23]. The approach based on the angular power spectrum and the estimator D defined in Eq. (2.1) did not allow

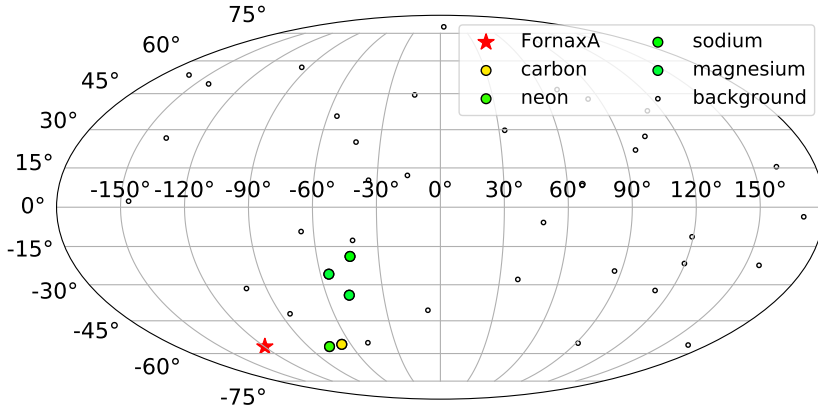


Figure 3. An example of five UHECRs with energies above 57 EeV coming from Fornax A that can be recognised by the suggested CNN on the background of 35 events distributed isotropically.

us to find an anisotropy from a nearby source even in case the total sample contains 50,000 events, which is close to the size of the Pierre Auger data set taking into account their field of view. To the contrary, the CNN presented above is able to distinguish a pattern of from-source events comprising a much smaller fraction. For example, it is able to find a pattern produced by UHECRs with energies above 8 EeV coming from Cen A if they constitute just 0.3% of the same sample, with the same cuts on α and β . This suggests applying the technique to the analysis of data of the existing experiments.

5 Conclusions

We have demonstrated how one can strongly improve the efficiency of an analysis of arrival directions of UHECRs using machine learning techniques. The basic idea is to train a classifier which discriminates samples generated assuming null and alternative hypotheses and to use the classifier output as a test statistics. Already a toy neural network introduced in Section 3 allows one to enhance the sensitivity of the analysis compared to the classical approach based on calculating the angular power spectrum. An application of models that involve pattern recognition such as the suggested deep convolutional neural network on a HEALPix grid gives a really qualitative enhancement in terms of sensitivity to deviations from an isotropic distribution of arrival directions. It was shown in particular that the method allows decreasing the minimal number of events necessary to identify a nearby source within the employed model by 2–4 times thus drastically decreasing technical demands and the required total exposure of an experiment like K-EUSO or POEMMA.

We emphasise the proposed method can be applied in more complicated tasks than the one discussed above. For instance, a non-uniform exposure of the celestial sphere with the existing experiments is not a problem here, since it can be easily taken into account when generating training and validation sets of data. Last but not least,

the presented version of a CNN is modest on computational resources allowing one to perform the whole analysis on an average desktop computer.

In the future, we plan to take into account uncertainties in the energy of detected UHECRs, which influence the spectrum and thus the shape of patterns formed by nuclei arriving from a source.⁴ We also plan to study how robust are the trained neural networks to uncertainties in our knowledge of the Galactic magnetic field and to consider other models of the GMF, namely a model by Pshirkov et al. [24] and a recent improvement of the Jansson–Farrar model suggested by Kleimann et al. [25]. Finally, it is interesting to check if a further improvement in recognizing patterns of arrival directions and thus identifying sources of UHECRs can be obtained by changing the energy threshold of events selected for the analysis and by incorporating information on the energy or the depth of maximum of registered events in a neural network. We believe the suggested approach opens new promising possibilities for studying anisotropy of ultra-high-energy cosmic rays and identifying their sources.

Acknowledgments

The development of the classification method and the architecture of corresponding deep convolutional neural network is supported by the Russian Science Foundation grant 17-72-20291. We acknowledge partial financial support from the Russian Foundation for Basic Research grant No. 16-29-13065. Some of the results in this paper were obtained using the HEALPix package [26].

References

- [1] J. Linsley, L. Scarsi and B. Rossi, *Extremely energetic cosmic-ray event*, *Physical Review Letters* **6** (May, 1961) 485–487.
- [2] M. Casolino, P. Klimov and L. Piotrowski, *Observation of ultra high energy cosmic rays from space: Status and perspectives*, *Progress of Theoretical and Experimental Physics* **2017** (12, 2017) .
- [3] P. Klimov, M. Casolino and the JEM-EUSO Collaboration, *Status of the KLYPVE-EUSO detector for EECR study on board the ISS*, in *Proceedings, 35th International Cosmic Ray Conference (ICRC 2017): Bexco, Busan, Korea, July 12-20, 2017*, p. 412, 2017, <https://pos.sissa.it/301/412/pdf>.
- [4] M. Casolino, A. Belov, M. Bertaina, T. Ebisuzaki and the JEM-EUSO Collaboration, *KLYPVE-EUSO: science and UHECR observational capabilities*, in *Proceedings, 35th International Cosmic Ray Conference (ICRC 2017): Bexco, Busan, Korea, July 12-20, 2017*, p. 368, 2017, <https://pos.sissa.it/301/368/pdf>.
- [5] G. K. Garipov, M. Y. Zotov, P. A. Klimov, M. I. Panasyuk, O. A. Saprykin, L. G. Tkachev et al., *The KLYPVE ultra high energy cosmic ray detector on board the ISS*, *Bull. Rus. Acad. Sci. Physics* **79** (2015) 326–328.

⁴We thank Olivier Deligny for attracting our attention to the point.

- [6] A. V. Olinto, J. Adams, R. Aloisio, L. Anchordoqui, D. Bergman and M. Bertaina, *POEMMA: Probe Of Extreme Multi-Messenger Astrophysics*, in *36th International Cosmic Ray Conference (ICRC2019)*, vol. 36 of *International Cosmic Ray Conference*, p. 378, Jul, 2019, [1907.06217](#).
- [7] A. V. Olinto, J. H. Adams, R. Aloisio, L. A. Anchordoqui, D. R. Bergman, M. E. Bertaina et al., *POEMMA: Probe Of Extreme Multi-Messenger Astrophysics*, in *Proceedings, 35th International Cosmic Ray Conference (ICRC 2017): Bexco, Busan, Korea, July 12-20, 2017*, vol. 301, p. 542, 2017, [1708.07599](#).
- [8] O. Kalashev, M. Pshirkov and M. Zotov, *Prospects of detecting a large-scale anisotropy of ultra-high-energy cosmic rays from a nearby source with the K-EUSO orbital telescope*, *Journal of Cosmology and Astroparticle Physics* **2019** (sep, 2019) 034–034.
- [9] M. Kachelrieß, O. Kalashev, S. Ostapchenko and D. V. Semikoz, *Minimal model for extragalactic cosmic rays and neutrinos*, *Phys. Rev.* **D96** (2017) 083006, [[1704.06893](#)].
- [10] M. A. Nielsen, *Neural networks and deep learning*. Determination Press, 2015.
- [11] J. Hülss and C. Wiebusch, *Search for signatures of extra-terrestrial neutrinos with a multipole analysis of the AMANDA-II sky-map*, in *Proceedings, 30th International Cosmic Ray Conference (ICRC 2007): Merida, Mexico, July 3–11 2007*, 2007, [0711.0353](#).
- [12] PIERRE AUGER collaboration, A. Aab et al., *Multi-resolution anisotropy studies of ultrahigh-energy cosmic rays detected at the Pierre Auger Observatory*, *Journal of Cosmology and Astroparticle Physics* **1706** (2017) 026, [[1611.06812](#)].
- [13] O. E. Kalashev and E. Kido, *Simulations of ultra high energy cosmic rays propagation*, *J. Exp. Theor. Phys.* **120** (2015) 790–797, [[1406.0735](#)].
- [14] M. S. Pshirkov, P. G. Tinyakov and F. R. Urban, *New limits on extragalactic magnetic fields from rotation measures*, *Phys. Rev. Lett.* **116** (2016) 191302, [[1504.06546](#)].
- [15] R. Alves Batista, A. Dundovic, M. Erdmann, K.-H. Kampert, D. Kuempel, G. Müller et al., *CRPropa 3—a public astrophysical simulation framework for propagating extraterrestrial ultra-high energy particles*, *Journal of Cosmology and Astroparticle Physics* **1605** (2016) 038, [[1603.07142](#)].
- [16] R. Jansson and G. R. Farrar, *A new model of the Galactic magnetic field*, *Astrophys. J.* **757** (Sept., 2012) 14, [[1204.3662](#)].
- [17] M. D. Zeiler, *ADADELTA: an adaptive learning rate method*, *CoRR* (2012) , [[1212.5701](#)].
- [18] Y. LeCun, B. Boser, J. S. Denker, D. Henderson, R. E. Howard, W. Hubbard et al., *Backpropagation applied to handwritten zip code recognition*, *Neural Computation* **1** (Dec, 1989) 541–551.
- [19] T. S. Cohen, M. Geiger, J. Koehler and M. Welling, *Spherical CNNs*, in *International Conference on Learning Representations*, p. 542, 2018, [1801.10130](#).
- [20] N. Perraudin, M. Defferrard, T. Kacprzak and R. Sgier, *DeepSphere: Efficient spherical convolutional neural network with HEALPix sampling for cosmological applications*, *Astron. Comput.* **27** (2019) 130–146, [[1810.12186](#)].

- [21] N. Krachmalnicoff and M. Tomasi, *Convolutional neural networks on the HEALPix sphere: a pixel-based algorithm and its application to CMB data analysis*, *Astron. Astrophys.* **628** (2019) A129, [[1902.04083](#)].
- [22] F. Chollet et al., “Keras.” <https://github.com/fchollet/keras>, 2015.
- [23] Pierre Auger Collaboration, A. Aab, P. Abreu, M. Aglietta, I. A. Samarai, I. F. M. Albuquerque et al., *Observation of a large-scale anisotropy in the arrival directions of cosmic rays above 8×10^{18} eV*, *Science* **357** (Sept., 2017) 1266–1270, [[1709.07321](#)].
- [24] M. S. Pshirkov, P. G. Tinyakov, P. P. Kronberg and K. J. Newton-McGee, *Deriving global structure of the Galactic magnetic field from Faraday rotation measures of extragalactic sources*, *Astrophys. J.* **738** (2011) 192, [[1103.0814](#)].
- [25] J. Kleimann, T. Schorlepp, L. Merten and J. Becker Tjus, *Solenoidal improvements for the JF12 Galactic magnetic field model*, *Astrophysical Journal* **877** (Jun, 2019) 76, [[1809.07528](#)].
- [26] K. M. Górski, E. Hivon, A. J. Banday, B. D. Wandelt, F. K. Hansen, M. Reinecke et al., *HEALPix: A framework for high-resolution discretization and fast analysis of data distributed on the sphere*, *Astrophys. J.* **622** (Apr., 2005) 759–771, [[astro-ph/0409513](#)].